EKMAN MASS AND HEAT TRANSPORT IN THE INDONESIAN SEAS

BY JANET SPRINTALL AND W. TIMOTHY LIU

The Indonesian throughflow (ITF) is the flow of warm, relatively fresh waters into the southeast Indian Ocean from the western Pacific Ocean via the series of passages between the islands of the Indonesian archipelago and Australia (see Figure 1 in Gordon, this issue). As the world's only low-latitude interocean conduit, the ITF plays an integral role in the global thermohaline circulation and directly impacts the basin heat and freshwater budgets of both the Pacific and Indian Oceans (Bryden and Imawaki, 2001).

We presently view the ITF as a low-frequency geostrophic flow combined with a surface wind-driven current (e.g., Meyers, 1996; Potemra et al., 1997). The large-scale steric height gradient between the easterly tradewinds in the western Pacific and the reversing monsoonal winds over the southern Indonesian seas drives the ITF's variable annual cycle (Wyrtki, 1987). During the northwest monsoon from November to March, the winds are to the southeast. The resulting Ekman flow causes warm waters to accumulate in the Banda Sea (Figure 1a), reducing ITF transport. The flow from the Banda Sea towards the Indian Ocean is strongest during the southeast monsoon from July to September when the winds are to the northwest and more intense, and the surface waters are cooler (Figure 1b). These strong winds result in a lower sea level along the south coast of the Nusa Tenggara island chain; the ITF is thought to be enhanced by this local Ekman response.

Although the geostrophic component and the total (ageostrophic plus geostrophic) ITF have been the subject of much historical and ongoing fieldwork in the Indonesian seas (e.g., Sprintall et al., 2004), the wind-driven Ekman contribution to the ITF has received relatively little attention. Arief (1992) observed a complex and inconsistent relationship between the east-west wind and the north-south current through Lombok Strait in which overall correlation was low, but strong events could be matched quite well. Murray and Arief (1988) explained the strong northward flow events observed in their northern current meters as being due to Ekman transport associated

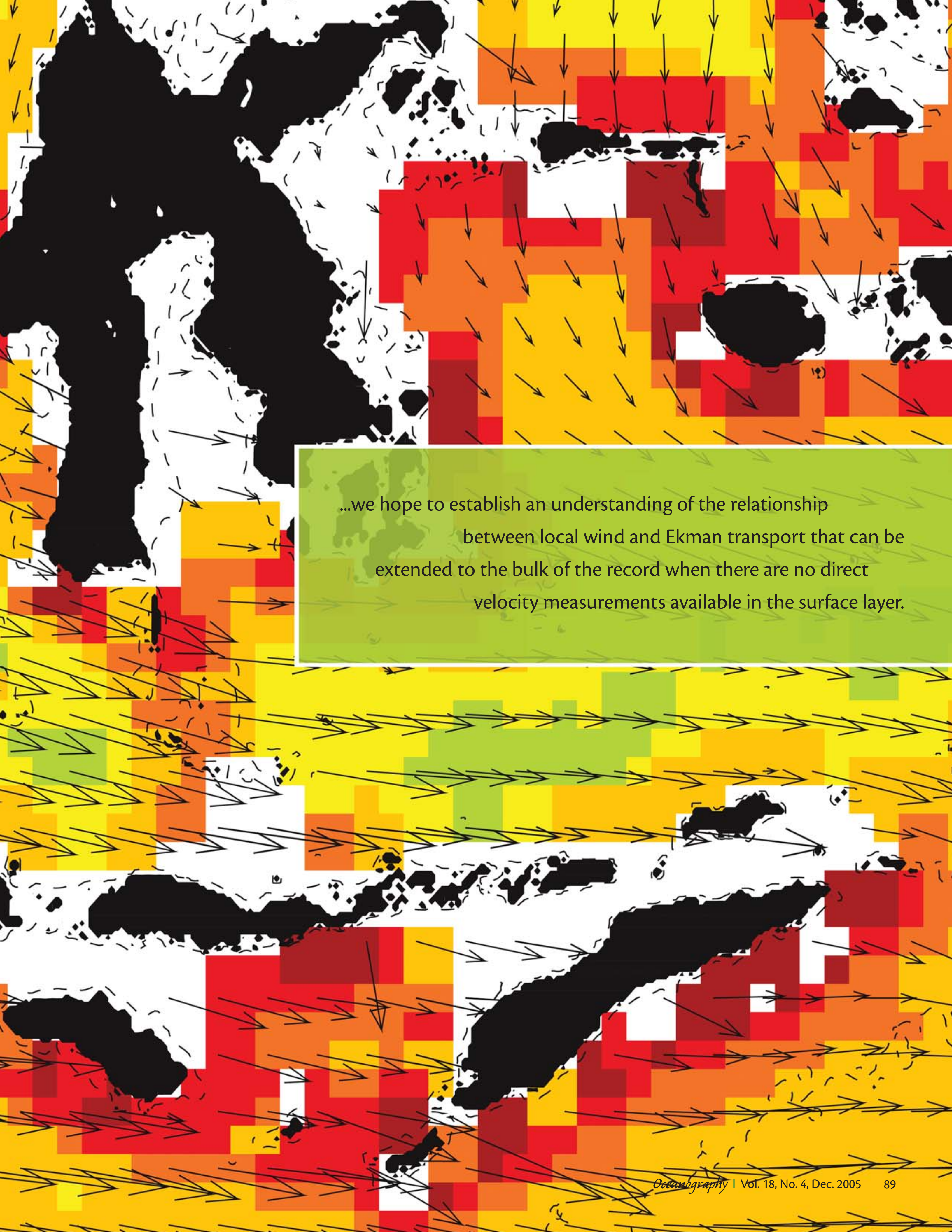

...we hope to establish an understanding of the relationship between local wind and Ekman transport that can be extended to the bulk of the record when there are no direct velocity measurements available in the surface layer.

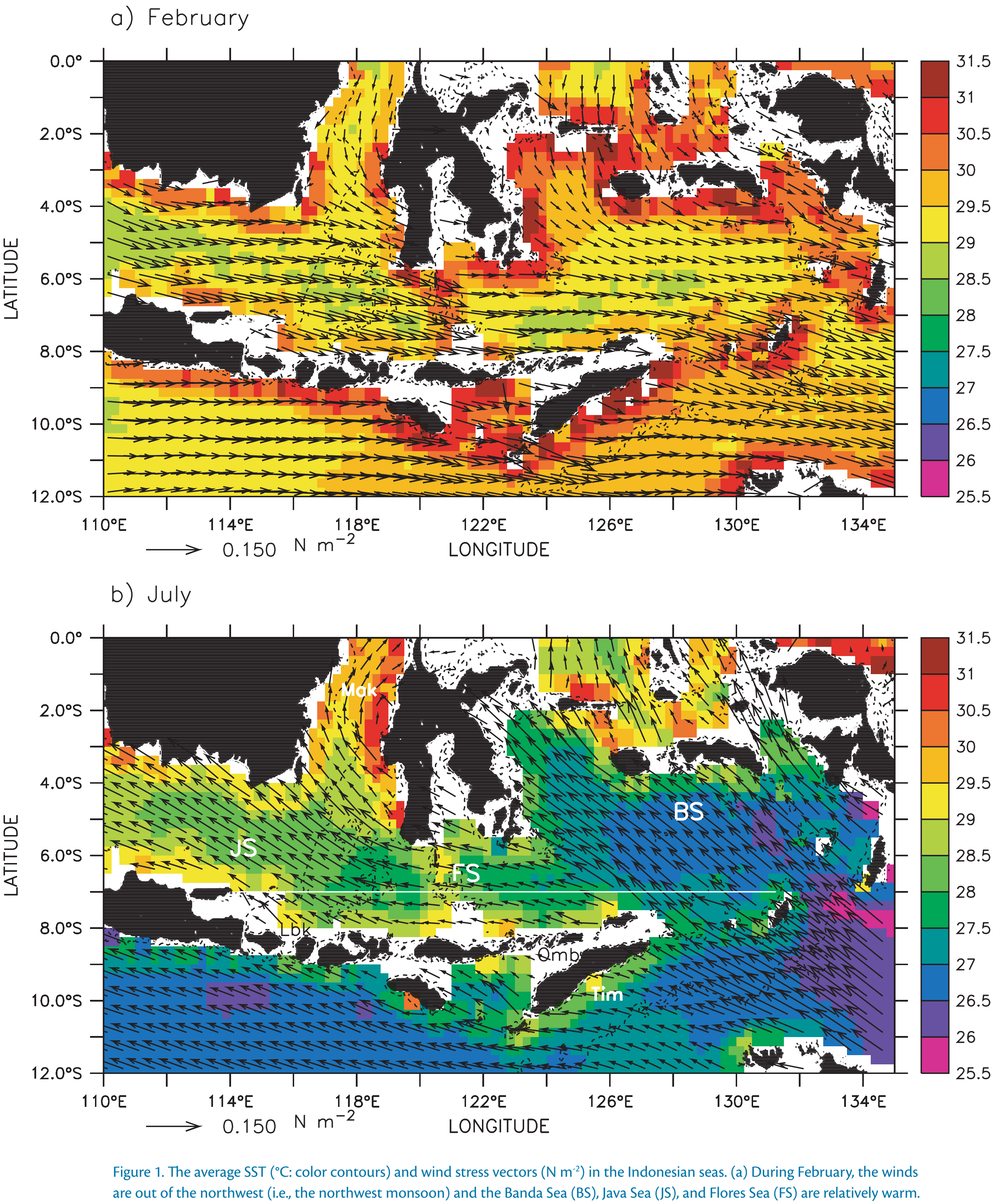

Figure 1. The average SST (°C: color contours) and wind stress vectors (N m^{-2}) in the Indonesian seas. (a) During February, the winds are out of the northwest (i.e., the northwest monsoon) and the Banda Sea (BS), Java Sea (JS), and Flores Sea (FS) are relatively warm. (b) During July, the winds are out of the southeast (the southeast monsoon), the internal seas are much cooler, particularly the Banda Sea. The Ekman mass and heat transports are calculated along the Nusa Tengarra transect (white line), which would capture flow that exits through Lombok (Lbk), Ombai (Omb), and Timor (Tim) passages into the Indian Ocean.

with cyclones passing westward through the center of the Indo-Australian Basin. More recently, northward flow in Lombok Strait has been linked to remotely forced Kelvin waves, particularly during the monsoon transition periods in November/December and April/May when equatorial Indian Ocean westerly wind events are most prominent (Sprintall et al., 1999, 2000). In Ombai Strait, Pandoe (2000) found that the time series from the second mode of an empirical orthogonal function (EOF) decomposition of the Ombai current meter data (Molcard et al., 2001) was significantly correlated with the local zonal wind stress. The temporal variability of the EOF mode 2 exhibited correspondence with the monsoonal signal in the zonal wind stress, with maxima in both time series occurring in January. In their thesis work, neither Arief (1992) nor Pandoe (2000) used the wind data to directly estimate the wind-driven Ekman flow in either Lombok or Ombai Straits. Using observed shipboard winds along two hydrographic sections during the southeast monsoon in August 1989, Fieux et al. (1994) estimated Ekman transports of –1.4 Sv toward the Indian Ocean between Australia and Bali, and –5.3 Sv between Bali and Timor, with –4 Sv estimated using climatological winds. Potemra et al. (1997) determined a similar average Ekman transport of –1.8 Sv toward the Indian Ocean along a transect between Java and Australia, with a strong seasonal cycle of ~5 Sv. Thus, it appears likely that at least on monsoonal time scales, surface-layer Ekman transport may contribute significantly to ITF transport.

There are no published estimates of the Ekman contribution to the heat transport through the Indonesian seas. Vranes et al. (2002) determined a mean heat transport of 0.43 (0.55) PW (in Petawatts, 1PW=10^{15}W) relative to 0° (3.4°) C for the Makassar Strait contribution to the ITF from mooring measurements, which is slightly lower than the 0.66–1.15 PW estimate of the ITF heat transport from modeling studies (Schneider and Barnett, 1997; Schiller et al., 1998; Gordon and McClean, 1999). Vranes et al. (2002) lacked velocity and temperature values for the surface layer, and hence had to extrapolate from the shallowest measurements (~110 m) to the sea surface using a variety of model profiles. Kraus and Levitus (1986) found that because of the high sea surface temperatures (SSTs) in the tropical Pacific, over half the heat flux there was attributable to the Ekman contribution. Given the high SSTs found in the Indonesian region (Figure 1), it is not unreasonable to assume that the Ekman heat flux may also play a substantial, but as yet undetermined, role in ITF heat transport.

In this paper, we use surface wind stress determined from scatterometer data and satellite-derived SST to provide the first estimates of the indirect Ekman mass and heat flux in the Indonesian seas. These remotely sensed fields are more accurate and have higher spatial resolution than climatology, and thus better resolve the various internal Indonesian seas.

Janet Sprintall *(jsprintall@ucsd.edu) is Associate Research Oceanographer, Scripps Institution of Oceanography, La Jolla, CA, USA.* **W. Timothy Liu** *is Principal Scientist, Jet Propulsion Laboratory/Caltech, Pasadena, CA, USA.*

DATA AND METHODS

The wind-based estimates of the meridional Ekman transport (M^y_{Ek}) are calculated from the along-track integral of the zonal wind stress (τ_x),

$$M^y_{Ek} = \int_{x2}^{x1} \frac{-\tau_x}{\rho f} dx \qquad [1]$$

where ρ is the average water density over the upper layer (assumed constant at 1025 kg m^{-3}), and f is the Coriolis parameter. The Ekman heat flux is then given by,

$$\Theta^y_{Ek} = -c_p \int_{x2}^{x1} \frac{\tau_x}{f} (\theta_e - \bar{\theta}) dx \qquad [2]$$

where c_p is the specific heat capacity of sea water at constant pressure (assumed constant and equal to 4000 J kg^{-1}°C^{-1}), θ_e is the Ekman layer potential temperature, and $\bar{\theta}$ is the mean potential temperature of the water column.

The zonal component of the wind stress (τ_x) was determined using vector wind measurements from the SeaWinds scatterometer on Quikscat. The wind stress product is based on an iterative procedure to evaluate the corresponding frictional velocity (Tang and Liu, 1996). These data are provided on a 0.25° grid for both ascending and descending passes, and available online at http://podaac.jpl.nasa.gov. All available data were averaged to form weekly fields from July 1999 to March 2005. We compared this field to the zonal wind stress derived using the familiar Large and Pond (1981) bulk parameterization of the wind-speed-dependent drag coefficients (not shown). Although the pattern of the two wind stress fields is the same, the Large and Pond (1981) has slightly smaller amplitude compared to Tang and Liu

(1996). In the following, we restrict our analysis to the Tang and Liu (1996) wind stress fields, although our conclusions remain the same for calculations using either wind stress product.

In this study we use SST as a first approximation to temperature of the Ekman layer (θ_e), following Kraus and Levitus (1986) and Levitus (1987), among others. We will discuss the deficiencies related to this approach in the Discussion. The Tropical Rainfall Measuring Mission (TRMM) Microwave Imager provided the first accurate retrievals of microwave SSTs that offer a distinct advantage over traditional satellite SST observations in the Indonesian region because the radiometer measures SST through clouds. We use the objectively analyzed weekly fields on a 0.25° grid, available from Remote Sensing Systems (http://www.ssmi.com) for the same period as the surface wind stress data (July 1999–March 2005).

The choice of a mean potential temperature ($\bar{\theta}$), often called the "reference temperature," should reflect the temperature of the deeper compensating transport that balances the Ekman layer transport given by [1]. In this sense, the system is then closed as mass is conserved. A number of choices of $\bar{\theta}$ have been discussed in the literature that are essentially average temperatures of the deeper flow (e.g., Vranes et al., 2002; Sato et al., 2002). In this study, a reasonable choice that lets us compare our results to the existing estimates of heat flux in the Indonesian region (Schneider and Barnett, 1977; Vranes et al., 2002) is a $\bar{\theta}$ of 3.4°C. This is the spatially averaged temperature of a meridional section between Australia and Antarctica, which is where most of the return flow into the Pacific Ocean must cross to eventually enter the ITF.

Finally, the longitudes of the integration limits in [1] and [2] are chosen for a transect that lies just north of the Nusa Tenggara island chain (referred to as the NT transect; Figure 1b). The transect lies between 115.125°E and 131.675°E between the islands of Madura, just north east of Java, and Tanimbar in the eastern Banda Sea. To maximize the available data, the values for SST and τ_x along this transect are averaged between 6.125° and 7.875°S. It is worth explicitly pointing out that if there were no passages along this island chain, then the wind-driven flow would just upwell or downwell against the coast, and thus not contribute mass or heat to the ITF. However, there are numerous passages along the Nusa Tenggara island chain, including Lombok, Ombai, and Timor Passages that are known to be major exit straits for the full-depth ITF into the Indian Ocean (Sprintall et al., 2004). Hence, this transect would capture most of the Ekman flow of the ITF between these islands.

VARIABILITY IN SST, WIND STRESS, EKMAN MASS, AND HEAT TRANSPORTS

Because Ekman fluxes are a product of the integration of SST and zonal wind stress, it is constructive to examine the variability of these quantities along the NT transect with time (Figure 2). The SST shows a strong semi-annual signal (Figure 2a), with maximum temperature occurring around November and a slightly lower maximum occurring in April of each year. These peaks in SST coincide with the monsoon transition periods when both the zonal (Figure 2b) and the meridional wind stresses (not shown) are near zero, so there is little wind-driven mixing and the air-sea heat input into the upper layer may be strong. The zonal wind stress variability is dominated by the two monsoons (Figure 2b). There is no distinct semi-annual signal as found in the SST.

Much stronger westward wind stress (Figure 2b) and cooler SST (Figure 2a) are found in the Banda Sea during the southeast monsoon period, compared to that found in the Java and Flores Sea to the west. During this monsoon, in the Banda Sea there is a two to three month phase lag between the strongest winds that occur around May and June and the coolest SST that occurs in July and August (Figure 2). The scenario is suggestive of cooling by the Ekman pumping that occurs during this monsoon in the Banda Sea (Gordon and Susanto, 2001).

In contrast to the stronger response evident in the Banda Sea region during the southeast monsoon (Figures 1 and 2), there is relatively little zonal variability in the magnitude of SST or zonal wind stress along the transect during the northwest monsoon. Slightly warmer SST is found in the relatively shallow region north of Flores Island from 120°E–123°E (Figure 1a). Highest SSTs occur when wind speeds are low or relaxed, with a relatively rapid cooling occurring during the strong episodic wind bursts that are more characteristic of the northwest monsoon: there is no temporal phase lag evident in the SST response to strong winds as found during the southeast monsoon (Figure 2). A secondary minimum in SST occurs around February each year coinciding with the strongest winds during the

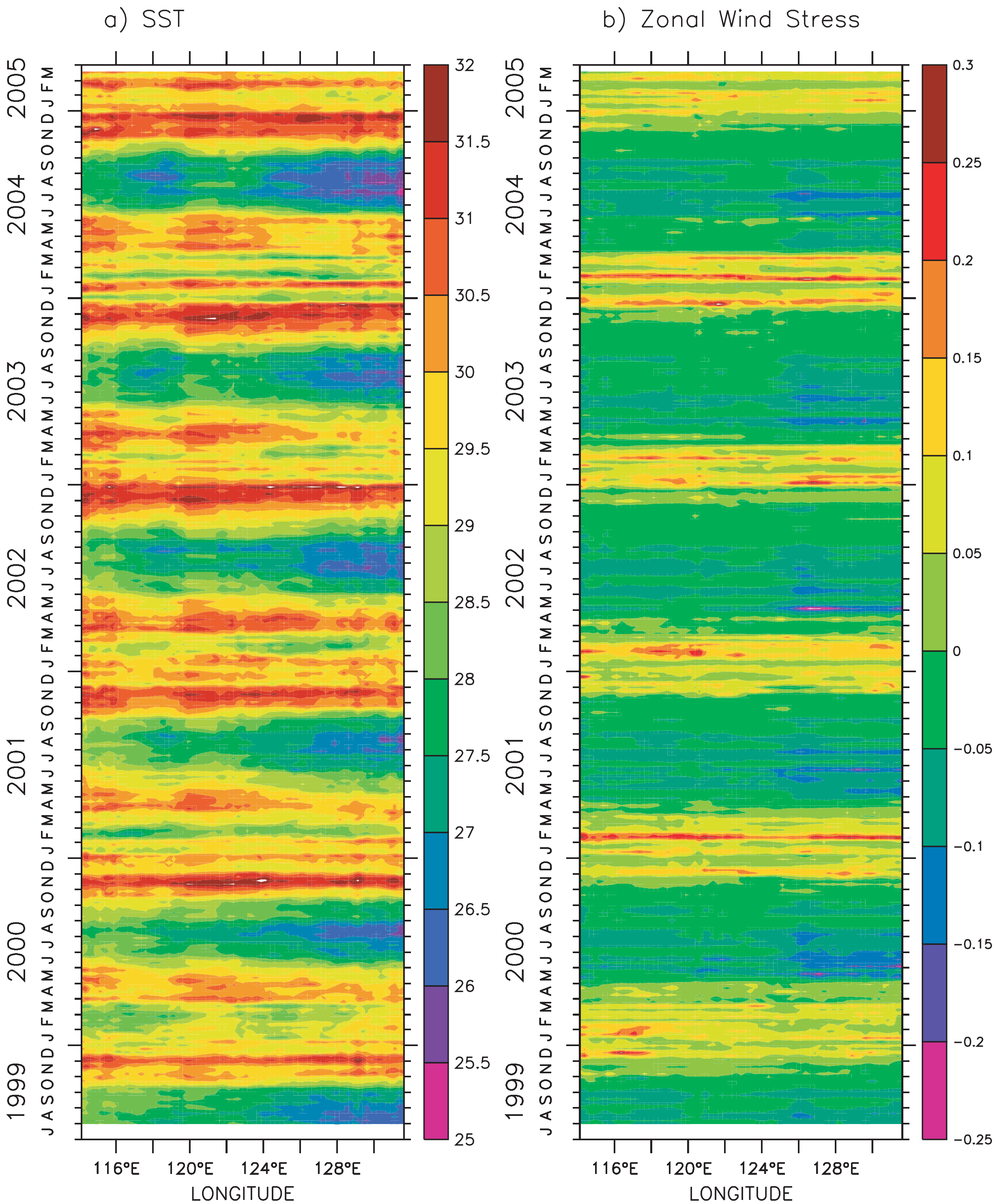

Figure 2. The (a) SST (°C) and (b) zonal wind stress (N m^{-2}) along the Nusa Tengarra transect at ~7°N (shown by the white line in Figure 1) from July 1999 through March 2005. Warmer SST and eastward (positive) wind stress occurs during the northeast monsoon from December through February. Cooler SST and westward wind stress occurs during the southeast monsoon from June through September, and is strongest in the Banda Sea region from 125°E to 131°E. Warmer temperatures also occur around November and April each year when the wind stress is small during the monsoon transitions.

northwest monsoon period. Given the rapid response, it is likely that the latent heat component of the air-sea flux plays a strong role in producing the cooler SSTs at these times. We also note a slight tendency for the warmer SSTs at the beginning of the northwest monsoon in October and November to occur first at the western end of the NT transect (Figure 2a). The difference in response of SST from west to east along the NT transect is in agreement with the arrival of the monsoon winds from the Indian Ocean to the west.

Finally, apart from the cooler SST during the 2004 southeast monsoon, there is surprisingly little difference in year-to-year variability of SST or zonal wind stress of the 5.5-year time series (Figure 2). Because of the strong coupling between the Pacific trade winds and the Indian Ocean monsoons (Webster et al., 1998), one might expect to see an interannual signal in the SST and wind stress time series related to El Niño-Southern Oscillation (ENSO) events, as noted, for example, in Makassar Strait transport and thermocline variability (Gordon et al., 1999; Ffield et al. 2000). Over the 5.5-year time series used in this study, a La Niña event that began in 1998 continued through the end of 2000, and a mild El Niño event began in 2004. In their study of variability in the Banda Sea using composite ENSO events, Gordon and Susanto (2001) suggest cooler (warmer) than average SST and weaker (stronger) than average Ekman pumping occurs during the southeast monsoon of El Niño (La Niña) events. Our results support this finding during the southeast monsoon of 2004 El Niño event (Figure 2), although it is less clear-cut during the 1998–2000 La Niña event. Figure 2 shows that during the southeast monsoon in 2000, the strongest southeasterly winds were relatively prolonged, but in contrast to Gordon and Susanto (2001), SST was near normal or slightly cooler than average. Warmer SST and stronger winds were found along the entire NT transect over the 2000–2001 northwest

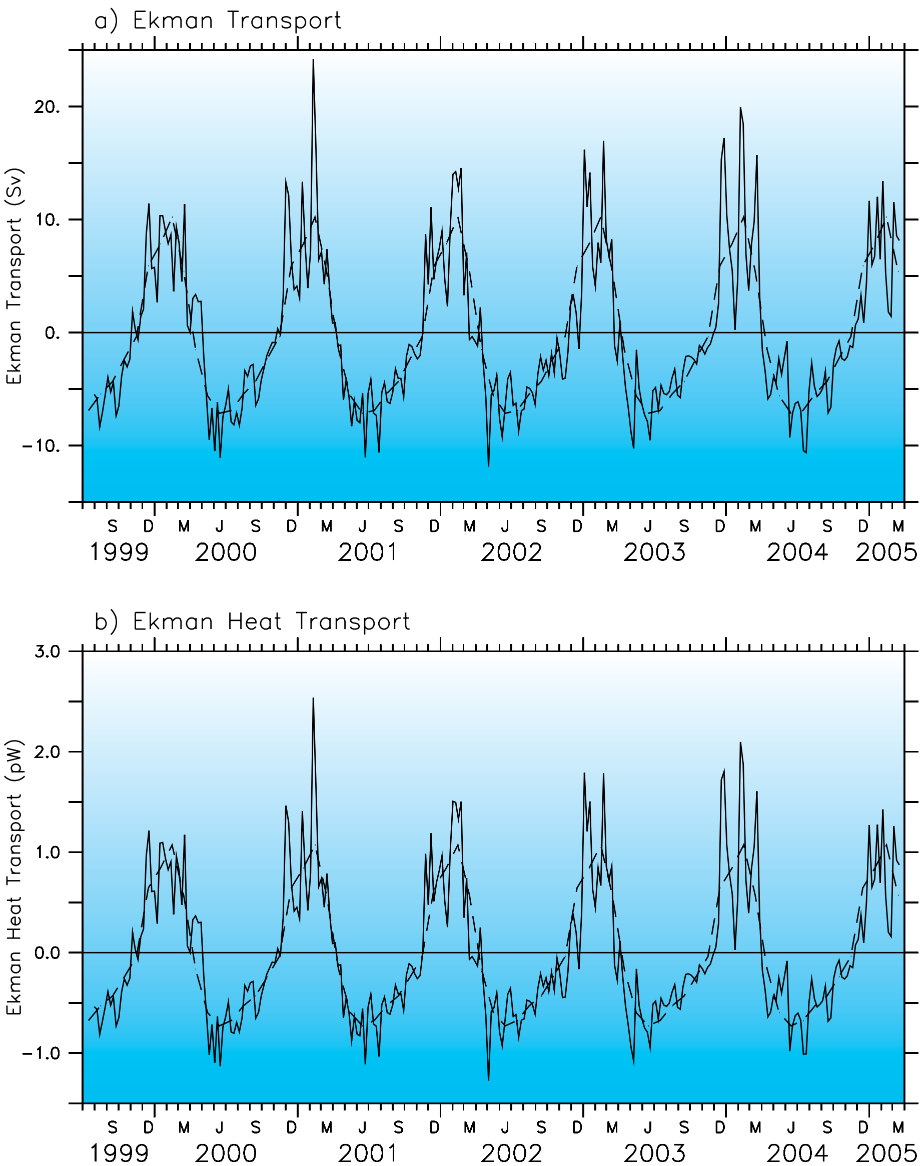

Figure 3. The (a) Ekman volume transport (Sv) and (b) Ekman heat transport (PW) integrated along the Nusa Tengarra transect at ~7°N (shown by the white line in Figure 1) are southward toward the Indian Ocean (negative values) during the southeast monsoon, with large episodic northward transports evident during the northwest monsoon. Both the Ekman volume and heat transports monthly averaged values (dashed lines) show similar seasonal cycles in response to the monsoonal changes in the wind stress.

monsoon period, however, this was when conditions were returning to near normal in the Pacific.

The time series of Ekman volume (Figure 3a) and heat transport (Figure 3b) clearly shows that changes in both fields are dominated by changes in the zonal wind stress field (Figure 2b). There is no semi-annual signal similar to that found in the SST field (Figure 2a) in either Ekman mass or heat transport (Figure 3). As expected, Ekman transport is to the south in mid-year when winds are to the west, and to the north over the new year when winds are to the east. The magnitude of the Ekman transport is surprisingly large. During the prolonged southeast monsoon, southward transport hovers around 5 Sv, while the strong, episodic wind events during the northwest monsoon lead to sporadic northward Ekman transports of ~10–15 Sv. These figures imply that at least on seasonal time scales, the Ekman contribution to ITF transport may be significant. For comparison, a time series from 1996–1999 of geostrophic transport through Lombok, Ombai, and Timor Passages, inferred from the cross-strait pressure gradient measured by coastal pressure gauges, shows a similar monsoonal seasonality to the Ekman transport in Figure 4, but the range in geostrophic transport was only –5 Sv to 7 Sv (Figure 11 of Hautala et al., 2001). In addition, Potemra et al. (2002) showed that the geostrophic transport variability is primarily due to remote wind-forced Kelvin waves from the Indian Ocean on intraseasonal to semi-annual time scales (Sprintall et al., 2000), and Pacific equatorial Rossby waves on interannual time scales. There is relatively little relationship between geostrophic transport variability and local wind forcing, a result also shown by Wijffels and Meyers (2004).

The pattern of Ekman heat transport (Figure 3b) closely mimics the Ekman volume flux (Figure 3a). This suggests that the $(\theta_e - \overline{\theta})$ term contributes little to the integration of equation [2]: most, if not all of the variability in Ekman heat flux is driven by changes in the Ekman volume transport. It may also be that (1) our choice of SST to represent the Ekman layer temperature is inappropriate (discussed further below) or (2) our choice for the reference layer temperature is inappropriate. With respect to (2), the assumption of mass conservation in equation [2] demands a high dependence upon a suitable choice of $(\overline{\theta})$ that is representative of the depth-average temperature of the compensatory return flow. As our results were relatively insensitive to a range of choices for $(\overline{\theta})$ from 0°C to 4°C, it is probable that a simple heat flux model such as equation [2], which horizontally and vertically evenly distributes the associated return flow and its temperature, does not allow for differences in flow contributions, for example, from boundary currents. Further, it neglects changes in temperature induced by surface heat exchange and, indeed, assumes no contribution of heat through the surface in the heat balance. Although it is beyond the scope of the present work, such processes should be carefully accounted for in a more comprehensive analysis of the Ekman contribution to the total ITF heat transport, and its resulting influence on the heat budgets of the Pacific and Indian Oceans.

Because of a varying strength in the winds during each of the two monsoon seasons, in some regions of the monsoon-affected Indian Ocean the amplitude of the annual wind stress cycle

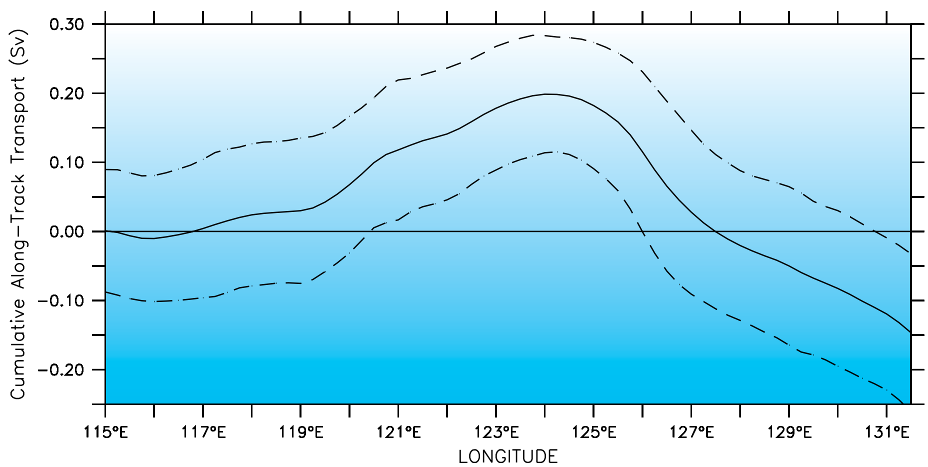

Figure 4. The horizontal distribution of the cumulative average (solid) Ekman transport (Sv) from west (115°E) to east (131°E) across the Nusa Tengarra island chain. The cumulative Ekman transport is southward toward the Indian Ocean to the east of 124°E, in response to the stronger southeast monsoons in this region, and hints that the contribution of Ekman transport through Ombai and Timor Passages may be significant. The standard deviation of the cumulative transport over the five-year record is shown by the dashed line.

is not symmetric about zero. Thus, we might expect to see a corresponding rectification of the net annual Ekman transport in relation to the season of strongest winds. However, even though the southeast monsoon is steadier and longer along the NT transect, because of the sporadic, strong westerly wind events during the northwest monsoon, the mean annual Ekman transport was only 0.35 Sv southward. For comparison, although the pressure gauge measurements are from a different time period, the mean geostrophic transport from 1996–1997 through the main Nusa Tenggara exit passages of Lombok, Ombai, and Timor Passages was 8.4± 3.4 Sv toward the Indian Ocean, which is in relatively good agreement with the mean total transport of ~8±2 Sv southward in Makassar Strait (Susanto and Gordon, 2005). Similarly, although the Ekman heat transport can vary between –0.8 to 1.0 PW on average (Figure 3b), the mean annual heat transport is only –0.023 PW. This is only ~6% of the total heat transport of ~0.4 PW that Vranes et al. (2002) determined for the Makassar ITF.

Although the long-term mean Ekman flux is small, the horizontal distribution shown by the cumulative mean Ekman transport across the NT transect suggests that some of the eastern passages may contribute to the total ITF mass and property transport into the Indian Ocean (Figure 4). This figure reflects the variation in the wind stress strength along the NT transect suggested in Figure 2. In the mean, northward transport occurs from Madira Island (at ~115°E) out to ~124°E, which nearly coincides with the eastern end of Alor Island to the north of Ombai Strait (Figure 1). East of 124°E to the end of the transect at Tamimbar Island (131°E), the cumulative transport across the section is southward (Figure 4) in response to the stronger southeast monsoon winds in this region (Figure 2), hinting that the contribution of Ekman transport to the ITF through Ombai and Timor Passages may be more significant.

DISCUSSION AND CONCLUSIONS

On monsoonal time scales, the wind-driven Ekman flow can contribute significantly to the ITF's total volume and heat transport through the exit passages into the Indonesian seas. The southward Ekman mass transport during the longer southeast monsoon is ~5 Sv, which is of the same order of magnitude as the geostrophic transport through Lombok, Ombai, and Timor Passages into the Indian Ocean during this monsoon phase. The Ekman heat transport is ~0.5 PW, similar to the total ITF heat transport through Makassar Strait (Vranes et al., 2002). However, in response to the stronger, but sporadic winds of the northwest monsoon, significant northward transport of ~10–15 Sv, with an associated Ekman heat transport of ~1 PW, occurs over this three-month period. Thus, the seasonal reversal of the winds means that on annual time scales and longer, the Ekman contribution to the total ITF is likely to be negligible. As in all measurements in the Indonesian region, this result confirms the need for caution interpreting Ekman transport estimates from short-duration measurements, such as "snap-shot" estimates from cruise data, as the observations may represent a significantly biased point of view.

Finally, we note that the Ekman mass and heat transports that are presented in this paper represent a first estimate of these quantities in the Indonesian seas. With more *in situ* data they can be improved and verified in many ways. For instance, these Ekman transports are "indirect" estimates as they are necessarily calculated using just the readily available wind stress data. "Direct" estimates of the ageostrophic Ekman flow and transport have been obtained by subtracting geostrophic currents estimated using hydrographic data from the total current determined from shipboard acoustic Doppler current profile (ADCP) measurements (Chereskin and Roemmich, 1991; Wijffels et al., 1994). The Ekman transport estimated in this way reveals the vertical structure of the wind-driven flow, its relation to the mixed layer, and of importance, its contribution to the heat and freshwater fluxes. If there is a significant temperature difference between the SST and the subsurface waters then this can have a profound influence on the Ekman fluxes if the wind-driven flow penetrates deeply. For instance, Chereskin et al. (2002) found the direct Ekman transport and transport-weighted Ekman temperature estimated from the surface to the top of the pycnocline from hydrographic/ADCP data collected along an Arabian Sea transect at the end of the monsoon in September 1995 were stronger and cooler than indirect estimates from wind and SST. However, along the same transect during June 1995 when the surface layer was strongly stratified, there was little difference between the indirect and direct Ekman estimates, and the transport-weighted Ekman temperature did not differ significantly from the surface value. At present, there are no concurrent *in situ* measurements available in the Indonesian region to determine the direct Ekman transport and true depth of wind-penetrating flow in the manner of Chereskin et al. (2002). However, with the expected recovery of the three-year measurements of surface layer velocity, temperature, and salinity from the INSTANT moorings in early 2007 (Sprintall et al., 2004), combined with the geostrophic estimate determined from the shallow pressure gauges that were concurrently deployed in the same ITF exit passages, we will have an unprecedented data set for determining the direct Ekman volume and heat transport of the ITF as it enters the Indian Ocean. The INSTANT measurements cover Lombok, Ombai, and Timor Passages, and hence will enable us to determine if indeed there are different Ekman contributions by the more eastern passages as hinted at by this study. Furthermore, the direct estimates from the INSTANT mooring data can be compared to the indirect Ekman estimates over the same period, such as were derived in this paper, using the highly accurate wind stress obtained from the high-resolution scatterometer data (Tang et al., 2005). In this way, we hope to establish an understanding of the relationship between local wind and Ekman transport that can be extended to the bulk of the record when there are no direct velocity measurements available in the surface layer.

REFERENCES

Arief, D. 1992. A study on low frequency variability in current and sea level in the Lombok Strait and adjacent region. Ph.D. Dissertation. Louisiana State University, Baton Rouge.

Bryden, H.L., and S. Imawaki. 2001. Ocean Transport of heat. In: *Ocean Circulation and Climate*, G. Seidler, J. Church and J. Gould, eds. Academic Press, Inc., London, U.K.

Chereskin, T.K., and D. Roemmich. 1991. A comparison of measured and wind-derived Ekman transport at 11°N in the Atlantic Ocean. *Journal of Physical Oceanography* 21:869–878.

Chereskin, T.K., W.D. Wilson, and L.M. Beal. 2002. The Ekman temperature and salt fluxes at 8°30'N in the Arabian Sea during the 1995 southwest monsoon. *Deep-Sea Research* 49:1,211–1,230.

Ffield, A., K. Vranes, A.L. Gordon, R.D. Susanto, and S.L. Garzoli. 2000. Temperature variability within Makassar Strait. *Geophysical Research Letters* 27:237–240.

Fieux, M.C., C. Andrie, P. Delecluse, A.G. Ilahude, A. Kartavsteff, F. Mantisi, R. Molcard, and J.C. Swallow. 1994. Measurements within the Pacific-Indian Oceans throughflow region. *Deep-Sea Research* 41:1,091–1,130.

Gordon, A.L., and J.L. McClean. 1999. Thermocline stratification of the Indonesian Seas—Models and observations. *Journal of Physical Oceanography* 29:198–216.

Gordon, A.L., and R.D. Susanto. 2001. Banda Sea surface-layer divergence. *Ocean Dynamics* 52:2–10.

Gordon, A.L., R.D. Susanto, and A.L. Ffield. 1999. Throughflow within Makassar Strait. *Geophysical Research Letters* 26:3,325–3,328.

Hautala, S. L., J. Sprintall, J. Potemra, A.G. Ilahude, J.C. Chong, W. Pandoe, and N. Bray. 2001. Velocity structure and transport of the Indonesian throughflow in the major straits restricting flow into the Indian Ocean. *Journal of Geophysical Research* 101:12,375–12,389.

Kraus, E.B., and S. Levitus. 1986. Annual heat flux variations across the tropical circles. *Journal of Physical Oceanography* 16:1,479–1,486.

Large, W.G., and S. Pond. 1981. Open ocean momentum flux measurements in moderate to strong winds. *Journal of Physical Oceanography* 11:324–336.

Levitus, S. 1987. Meridional Ekman heat fluxes for the world oceans. *Journal of Physical Oceanography* 17:1,484–1,492.

Meyers, G. 1996. Variations of the Indonesian throughflow and the El Niño-Southern Oscillation. *Journal of Geophysical Research* 101:12,411–12,420.

Molcard, R., M. Fieux, and F. Syamsudin. 2001. The throughflow within Ombai Strait. *Deep-Sea Research* I 48:1,237–1,253.

Murray, S.P., and D. Arief. 1988. Throughflow into the Indian Ocean through Lombok Strait: January 1985–January 1986. *Nature* 333:444–447.

Pandoe, W.W. 2000. Flow pattern in the Ombai Strait Indonesia, and its relationship with the Indonesian throughflow. Master of Science Thesis. Texas A&M University, College Station, 87 pp.

Potemra, J.T., S.L. Hautala, J. Sprintall and W.W. Pandoe. 2002. Interaction between the Indonesian seas and the Indian Ocean in observations and numerical models. *Journal of Physical Oceanography* 32:1,838–1,854.

Potemra, J.T., R. Lukas, and G.T. Mitchum. 1997. Large scale estimation of transport from the Pacific to the Indian Ocean. *Journal of Geophysical Research* 102:27,795–27,812.

Sato, O.T., P.S. Polito, and W.T. Liu. 2002. Intra-decadal variability in the Ekman heat flux from scatterometer winds. *Geophysical Research Letters* 29:17, 1831, doi:10.1029/2002GL014775.

Schiller, A., J.S. Godfrey, P.C. McIntosh, G. Meyers, and S. Wijffels. 1998. Seasonal near-surface dynamics and thermodynamics of the Indian Ocean and Indonesian throughflow in a global ocean general circulation model. *Journal of Physical Oceanography* 28:2,288–2,312.

Schneider, N., and T.P. Barnett. 1997. Indonesian Throughflow in a coupled general circulation model. *Journal of Geophysical Research* 102:12,341–12,358.

Sprintall, J., S. Wijffels, A.L. Gordon, A. Ffield, R. Molcard, R.D. Susanto, I. Soesilo, J. Sopaheluwakan, Y. Surachman, and H.M. van Aken. 2004. A New International Array to Measure the Indonesian Throughflow: INSTANT. *EOS Transactions* 85(39):369–376.

Sprintall, J., A. Gordon, R. Murtugudde, and D. Susanto. 2000. An Indian Ocean Kelvin wave observed in the Indonesian seas in May 1997. *Journal of Geophysical Research* 105:17,217–17,230.

Sprintall, J., J.C. Chong, F. Syamsudin, W. Morawitz, S. Hautala, N. Bray, and S. Wijffels. 1999. Dynamics of the South Java Current in the Indo-Australian Basin. *Geophysical Research Letters* 26:2,493–2,496.

Susanto, R.D., and A.L. Gordon. 2005. Velocity and transport of the Makassar Strait throughflow. *Journal of Geophysical Research* 110:C01005, doi: 10.1029/2004JC002425.

Tang, W., and W.T. Liu. 1996. Objective interpolation of scatterometer winds. *JPL Publication* 96–19, Jet Propulsion Laboratory, Pasadena, 16 pp.

Tang, W., W.T. Liu, and B.W. Stiles. 2004. Evaluation of high-resolution ocean surface vector winds measured by QuikSCAT scatterometer in coastal regions. *IEEE Transactions Geoscience and Remote Sensing* 42:1,762–1,769.

Vranes, K., A.L. Gordon, and A. Ffield. 2002. The heat transport of the Indonesian throughflow and implications for the Indian Ocean Heat Budget. *Deep-Sea Research* 49:1,391–1,410.

Webster, P., V. Magana, T. Palmer, J. Shukla, R. Tomas, M. Yanai, and T. Yasunari. 1998. Monsoons: Processes, predictability, and the prospects for prediction. *Journal of Geophysical Research* 103:14,451–14,510.

Wijffels, S.E., and G. Meyers. 2004. An intersection of oceanic waveguides: Variability in the Indonesian throughflow region. *Journal of Physical Oceanography* 34:1,232–1,253.

Wijffels, S.E., H.L. Bryden, and E. Firing. 1994. Direct observations of the Ekman balance at 10°N in the Pacific. *Journal of Physical Oceanography* 24:1,666–1,679.

Wyrtki, K. 1987. Indonesian throughflow and the associated pressure gradient. *Journal of Geophysical Research* 92:12,941–12,946.